 doi:10.20944/preprints202007.0671.v1

# FABRICATION AND CHARACTERIZATION OF LIGNIN/DENDRIMER ELECTROSPUN BLENDED FIBER MATS

Somaye Akbari[1*], Addie Bahi[2], Ali Farahani[1], Abbas S. Milani[3], Frank Ko[2*]

[1] Textile Engineering Department, School of Materials and Advanced Processes Engineering, Amirkabir University of Technology (Tehran Polytechnic), Tehran, Iran
[2]Department of Materials Engineering, University of British Columbia, Vancouver, BC, Canada
[3]School of Engineering, University of British Columbia, Kelowna, BC, Canada

Corresponding co-authors: Somaye Akbari (akbari_s@aut.ac.ir) & Frank Ko (frank.ko@ubc.ca)

**Abstract:** Blending lignin as the second most abundant polymer in nature with nanostructured compounds such as dendritic polymers will not only add value to lignin, but also increase its application in various fields. In this study, softwood Kraft lignin/polyamidoamine dendritic polymer (PAMAM) blends were fabricated by solution electrospinning method to produce bead-free nanofiber mats. The mats were characterized by scanning electron microscopy (SEM), contact angle measurement, Fourier transform infrared (FTIR), zeta potential, and thermogravimetry analysis (TGA). The chemical intermolecular interactions between lignin functional groups and abundant amino groups in PAMAM were investigated by FTIR and viscosity measurement. These interactions enhanced the mechanical and thermal characteristics of lignin/PAMAM mats, providing further potential applications at industry level.

Preprints (www.preprints.org) | NOT PEER-REVIEWED | Posted: 28 July 2020 doi:10.20944/preprints202007.0671.v1

## 1. Introduction

Lignin is one of the complex natural polymers that mostly exists in the by-product of plants, woods, pulp, and paper [1, 2]. It is a biopolymer with an irregular network which has made up three main units linked together with carbon-carbon bonds [3]. Lignin contains an aromatic structure with a phenolic ring in its precursors' monomer that mainly classified into three monomer units of coniferyl alcohol (G), p-coumaryl alcohol (H), and sinapyl alcohol (S) [4-7]. Softwood lignin existed in gymnosperm plants commonly consists of 24-33% of the cell wall [1], of which nearly 95% is G-lignin [8]. The various structure of functional groups in lignin comes from the type of plant and extraction methods [9]. The number-average molecular weight ($M_N$) between 3000 and 10000 and weight-average molecular weight ($M_W$) of 8000 to 80000 are very common for lignin depending on its type and other effective parameters [10]. Besides various structure and type of lignin products, they reveal some characteristics, such as antioxidant, antiseptic, bactericide, bacteriostatic, and disinfectant agent; whilst, its non-cytotoxicity toward human cells [11, 12]. These characteristics increase the productions and demands on lignin based products. For instance, in 1998, only 1% of lignin was isolated and sold [13]; whilst, in 2017, there were almost 70 million tons of wood pulping operation in worldwide of which 30 wt.% was extracted lignin [14].

One of the advantages of using lignin products is its renewable resource of carbon due to phenolic structure [15]. Thus, a wide range of lignin based products in the form of powders and/or fibers utilized as additives in composite products [1, 16]. The mechanical and thermal properties of the composite structures can improve when lignin is grafted or blended with other polymers, such as polypropylene (PP) as a cross-linker [17], polybutadiene (PB) and PP as an antioxidant [18], polyaniline as a conductivity modifier [19] and starch materials as a hydrophobic co-plasticizer [20]. However, much remains to research to find out the higher ability and new applications for lignin [21]. Lignin has also used as an anti-UV Stabilizer due to its phenolic and other organic structure and three-dimensional network of hydroxyl groups [22]. Besides on its novel characteristics and structure, lignin has also disadvantages, such as hydrophobic behavior [23], small particle size and variation in adhesion properties for coating composite structures, and extensive thermal behavior and $T_g$ range because of its complicated structures [24], and content condensation during extraction and production [25]. Due to these disadvantages, researchers have aimed to improve lignin characteristic by surface modifications or bulk modifications [26]. One of the novel techniques for modification of lignin-based products is blending with other polymers, such as dendritic structure polymers.

Dendritic structures have high potentials due to their special design, novel characteristics particularly host-guest properties, and nano dimension structures. They have formed from small repeating units, named generation numbers, onto the a central core to which other branches link and make a macromolecular structure with novel structure and characteristics [27]. The most outstanding characteristic, host-guest properties, comes from large numbers of functional reactive end-groups as well as hollow interior cavities between branches. The unique

 doi:10.20944/preprints202007.0671.v1

characteristic of dendrimers is their branched topology and multifunctional reactive groups [28]. One of the well-known dendrimers is polyamidoamine (PAMAM) dendrimer which provides amine-terminated functional groups with various kinds of applications. In this paper, PAMAM was blended with softwood kraft lignin and electrospun fibers to achieve new improvements for the first time.

Electrospinning is an efficient method for fabricating fibers in nano and micro-scale [29]. Thus, it is believed that electrospinning of lignin with other polymers can provide opportunities to achieve new characterizations resulting new applications [30]. For instances, electrospun lignin can be used for carbon fiber production [31-34], filtration membranes [35], biorefinery processes [36], biomedical and drug delivery applications [37], and wood panel products [38]. Various parameters, such as surface tension, viscosity, and electrical conductivity are affected on to the lignin nanofiber production [39]. Due to the chemical structure and properties of lignin, it has been blended with other polymers, such as polyethylene oxide (PEO) [40], polyvinyl alcohol (PVA) [41], polyacrylonitrile (PAN) [32], and polyethylene terephthalate (PET) [42]. Blended polymers help lignin to become spinnable fiber due to their good miscibility.

In order to improve the mechanical properties of electrospun lignin fiber particularly due to swelling in water, the fiber is heat-set or thermo stabilized [43]. In heat-setting process physical property changes like the color of lignin mats, which transforms from light yellow to dark brown, and the chemical reactions such depolymerization, recondensation would occur after increasing the temperature [44]. Lignin has also potential to participate in condensation reaction with fragments and side chain cleavage of ether linkage occur [43]. Besides, decreasing phenolic bond and forming new reactions would produce higher molecular weight in heat-setting processes; While, in stabilization process there are higher temperatures than heat-set process in order to achieve a sample with high strength and modulus [44].

The aim of this paper is to evaluate the fabrication and characterization of a novel blending between PAMAM dendritic structure and softwood kraft lignin (SKL). Furthermore, the heat-setting and stabilization process of SKL nanofibers are analyzed in the presence of PAMAM polymers. The interaction between lignin and PAMAM dendrimers are studied by FTIR, TGA, mechanical properties, surface charge, and viscosity measurement. In addition, the morphology of all samples is determined by SEM analysis. Overall, the results to follow confirmed the novel characteristics of lignin/PAMAM electrospun fibers which would make it a good candidate for further applications.

## 2. Results and Discussion

### *2.1 Morphology analyses*

The SEM images of electrospun lignin, lignin/PAMAM (1wt%) and lignin/PAMAM (2wt%) showed in Fig. 1. It must be noted that after increasing the concentration of dendrimer from 1% to 2wt%, it is not possible to continue the process of electrospinning. The optimum concentration

Preprints (www.preprints.org) | NOT PEER-REVIEWED | Posted: 28 July 2020 doi:10.20944/preprints202007.0671.v1

of PAMAM in this blending was 1% and other experiments applied on lignin/PAMAM with 1wt% of PAMAM. As a result, the abbreviation of lignin/PAMAM in all text means 1wt% of PAMAM based on the lignin weight. By increasing the PAMAM concentration, the viscosity of the main solution reduced. Thus, the fiber fabrication is impossible. This behavior for other polymers has been also elucidated by other investigators [45].

(a) (b) (c)

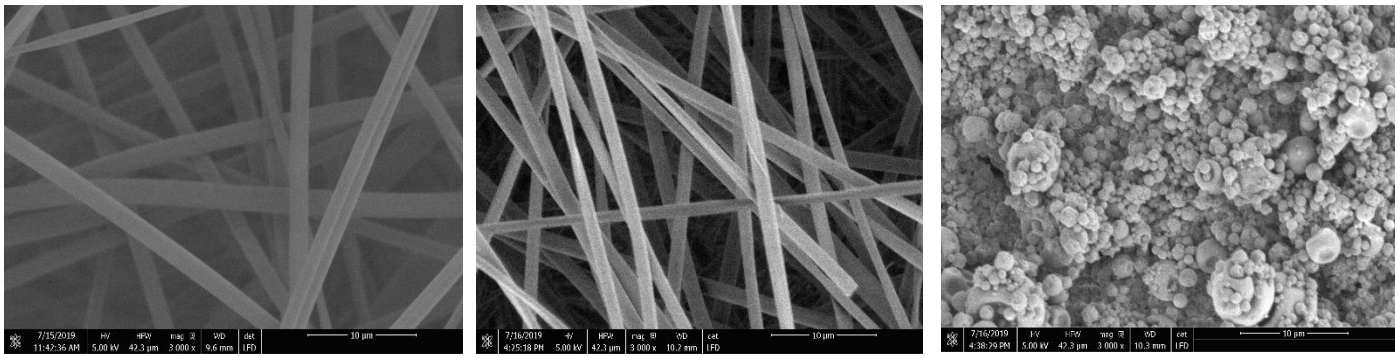

**Figure 1**. SEM of (a) lignin; (b) lignin/PAMAM 1wt%; (c) lignin/PAMAM 2wt%

The fiber diameters of lignin and lignin/PAMAM were measured before and after thermal-treatment (Heat-set) using SEM, as illustrated in Fig. 2. It is observed that the average diameter of the lignin/PAMAM nanofibers in both heat-set and not heat-set samples was less than the pristine lignin nanofibers due to the reduction of surface tension in electrospinning procedure by cationic charges of PAMAM polymers. PAMAM could act as a poly-electrolyte and reduce the diameter of electrospun fiber [46]. In addition, chemical interaction between cationic functional groups of PAMAM and anionic hydroxyl groups in lignin could be another reason for decreasing at about 10 percentage of the fiber diameter. On the other hand, as shown in Table 1, the total average diameter of both lignin and lignin/PAMAM nanofibers has been reduced after heat-setting process due to dehydration and possible reaction of the hydroxyl group in lignin and lignin/PAMAM. This diameter reduction after heat-setting processes can be as a result of the depolymerization, recondensation processes [44].

*Preprints* (www.preprints.org) | NOT PEER-REVIEWED | Posted: 28 July 2020 doi:10.20944/preprints202007.0671.v1

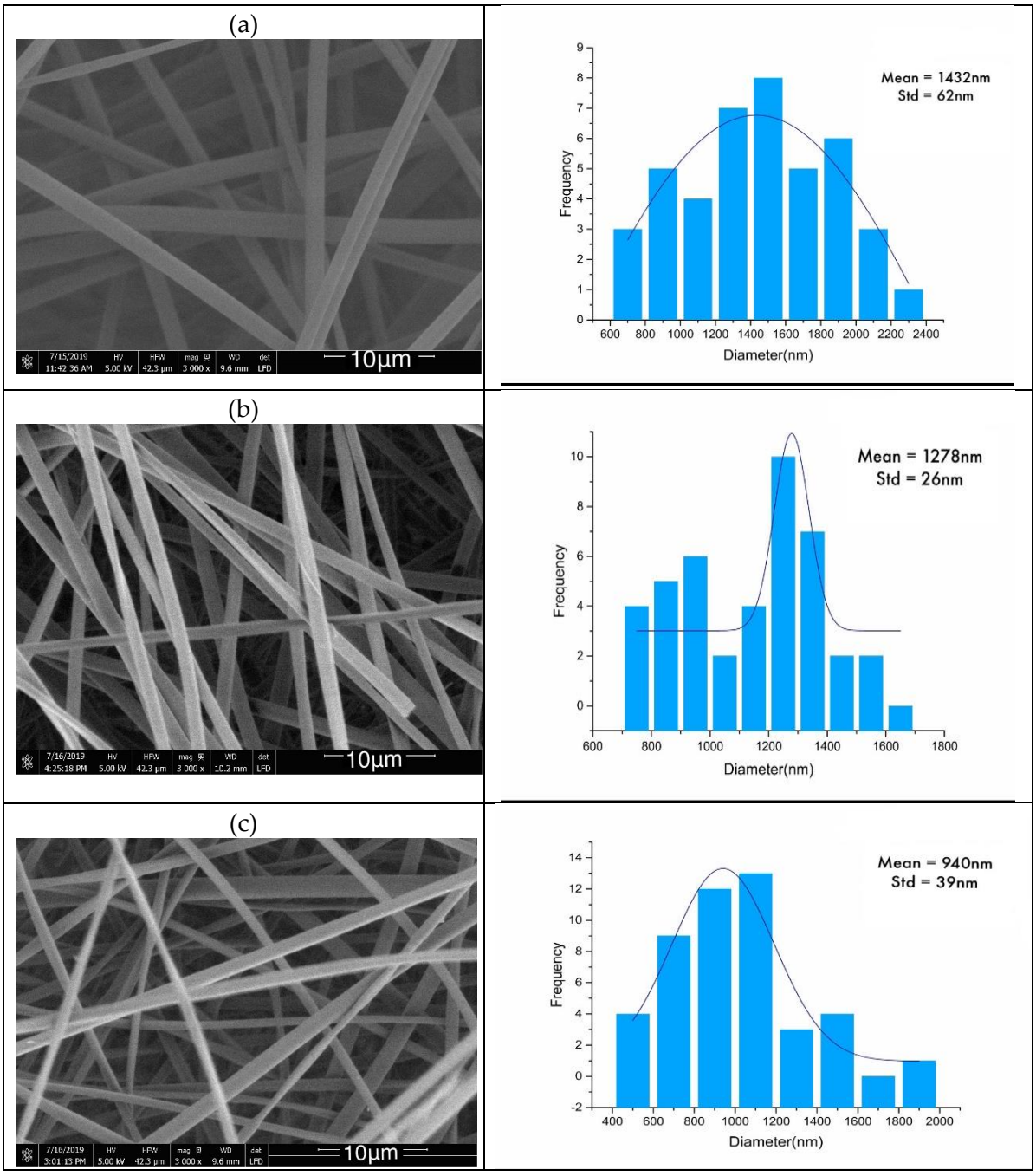

Preprints (www.preprints.org) | NOT PEER-REVIEWED | Posted: 28 July 2020 doi:10.20944/preprints202007.0671.v1

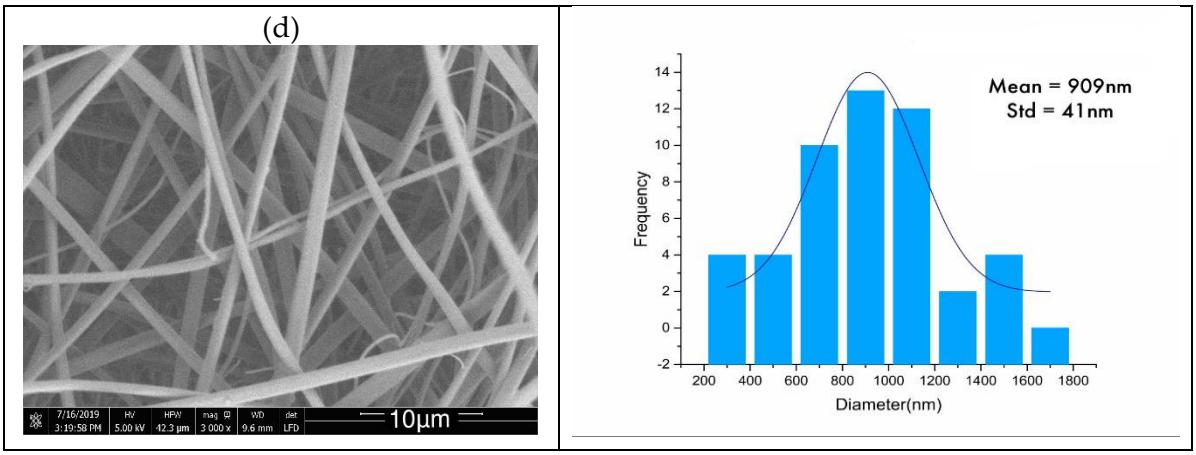


**Figure 2.** SEM of (a) lignin, (b) lignin/PAMAM, (c) heat-set lignin, (d) heat-set lignin/PAMAM, along with the corresponding fibre dimeter distributions.

Fig. 3 reveals the SEM images of lignin and lignin/PAMAM after thermostabilization processes (TSP). The TSP commonly used to prepare the carbon nanofibers (CNF) [47]. In this processes, higher temperature comparing to heat-setting processes causes more diameter reduction. The condensation procedure between amino terminated groups of PAMAM (−$NH_2$) and hydroxyl groups lignin (−OH) not only reduce the fiber diameter but also make a strong interaction between dendritic groups and lignin structure.

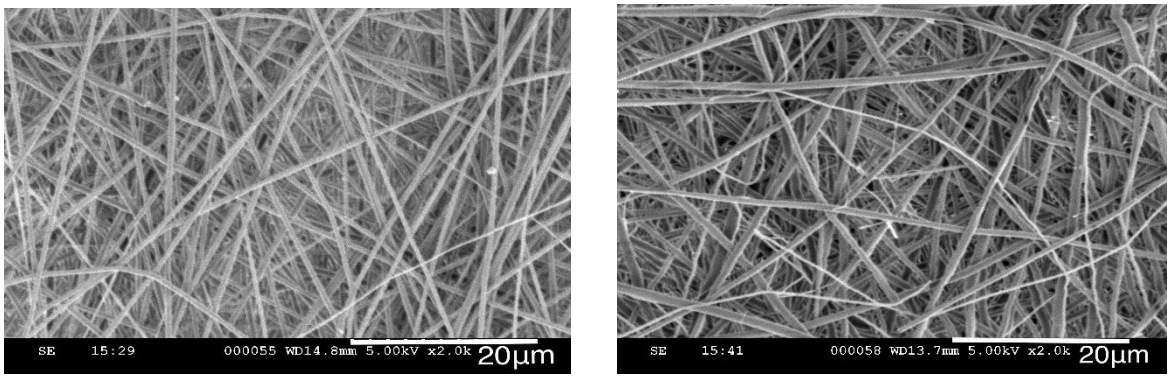


(a) (b)

**Figure 3.** SEM of (a)Lignin Stabilized, (b)Lignin/PAMAM Stabilized

**Table 1.** The average fiber diameter of electrospun lignin and lignin/PAMAM at the state of untreated, heat-setting, and stabilized in nanometer (nm).

| Sample | Untreated (nm) | Heat-set (nm) | Stabilized (nm) |
|---|---|---|---|
| Lignin | 1432±62 | 940±39 | 622±21 |
| Lignin/PAMAM | 1278±26 | 909±41 | 866±29 |

Preprints (www.preprints.org) | NOT PEER-REVIEWED | Posted: 28 July 2020 doi:10.20944/preprints202007.0671.v1

*2.2 Mechanical properties*

Mechanical properties of electrospun mats with and without PAMAM before and after heat-setting processes were evaluated. According to the heat treatment condition in each part of the process, as shown in Table 2, the maximum stress at yield point ($\sigma_y$) and elastic moduli (E) of the both lignin heat-set and lignin/PAMAM heat-set nanofibers reduced. While some researchers revealed tenacity enhancement of lignin electrospun fiber after heat-setting procedure due to the more cross-linking and chemical interaction between molecular chains in lignin based polymers [43, 44], other researchers elucidated tenacity reduction because of becoming more brittle [48]. It seems the process conditions, such as heating temperature, time of heating, and applied pressure have direct effect on the mechanical properties. However, almost all investigators have agreed that the heat-setting improve durability, biological behavior, and the dimensional stability [49].

Although there was an approximately sharp drop in the stress-strain curve in heat-setting processes, the effect of PAMAM on both heat-set and untreated mats was significant. As shown in Table 2, both ($\sigma_y$) and (E) increased. As a result, the fibrous mats of lignin/dendrimer were stronger the pristine samples and elastic recovery in both blended sample improved completely. The phenolic compounds and hydroxyl groups in lignin chemical structure react with functional groups of PAMAM; thus, the blended mats were much stronger and could tolerate more stress at high tension. The strong interaction between amino terminated groups of PAMAM ($-NH_2$) in dendritic groups and hydroxyl groups in lignin($-OH$) is the main reason for increasing the stress at yield and elastic moduli for lignin/PAMAM comparing to lignin electrospun fiber mats.

**Table 2.** Mechanical properties of the untreated lignin nanofiber mats.

| | untreated lignin nanofiber mats | | heat-set lignin nanofiber mats | |
|---|---|---|---|---|
| | Lignin | Lignin/PAMAM | Lignin | Lignin/PAMAM |
| Stress at yield ($\sigma_y$) (MPa) | 4.52±0.97 | 6.30±1.70 | 2.23±0.41 | 4.47±0.56 |
| Strain(%) | 5.68±1.54 | 6.73±2.67 | 5.17±1.28 | 7.02±1.96 |
| Elastic moduli (E) (MPa) | 79.66±1.01 | 93.61±1.73 | 43.19±0.68 | 63.72±0.74 |

*2.3 Surface charge*

Zeta potential can provide important information about surface chemistry and surface charge of electrospun mats, which is useful for various applications, such as water treatment, pharmaceutical, environmental protection, paint industry, and other applications [50]. Zeta potential describes the electrical charge and interactions of small particles at the surface which are dispersed in a material and can indicate the physical stability of the system in different states.

Preprints (www.preprints.org) | NOT PEER-REVIEWED | Posted: 28 July 2020 doi:10.20944/preprints202007.0671.v1

In addition, zeta potential can assist to reduce surface energy and optimize many related processes [51, 52].

In this research, lignin nanofiber mats were blended with PAMAM and the surface electrical charge was measured with the specific device for measuring surface charge of electrospun mats. The surface electrical charge of lignin is completely negative due to abundant hydroxyl and phenolic compounds in its structure as well as hydrogenation and decarbonylation alkyl groups [53]. While, the $NH_3^+$ groups in PAMAM reveals the positive zeta potential. The zeta potential of lignin was measured in the range of -23.28 mV, while it increases to -20.72 mV after adding 1% PAMAM based on the lignin weight. This increasing data confirms that only 1wt% of PAMAM lead to reacts between amine groups in PAMAM with some negative hydroxyl groups of lignin by more electrostatic interaction between lignin and PAMAM leading to high elastic moduli in tensile test for lignin/PAMAM mats comparing to lignin ones. Dallmeyer et. al [34] also revealed that inter-fiber bonding significantly enhanced the mechanical properties of the electrospun fabrics.

*2.4 Thermogravimetric analysis (TGA)*

The Thermogravimetry (TG) or Thermogravimetric Analysis (TGA) and Derivative thermogravimetry (DTG) curves of lignin and lignin/PAMAM before and after heat treatment (heat-set) are shown in Fig. 4a and b, respectively. The main characteristic and important peaks and information from these analyses are illustrated in Table 4. Lignin's main mass loss peak (according to its type and extraction) commonly appears at about 370-395 ˚C. While, the first peak appear in range of 150-270 ˚C corresponding to phenolic compounds of lignin [54]. The weight loss before 150 ˚C is due to the evaporation of water and small amount of dehydration reaction. At 380˚C, there is a peak related to hydrogenation of methoxy groups on the aromatic ring and consequently the evolution of methanol. Methane is another product that can release which starts at 350 ˚C and ends in 420-430 ˚C. Furthermore, carbon dioxide ($CO_2$) could release from 200 ˚C to 640-690 ˚C. Carbon monoxide (CO) also releases from 220 ˚C to 790 ˚C due to decarbonylation react of alkyl side-chain carbonyl terminate and the reaction of formaldehyde with free-radical coupling reactors in lignin [55, 56].

The results revealed that the weight of residue left by the lignin/PAMAM blended fiber mats was higher than that of pristine lignin in both untreated and heat-set (HS), as shown in Table 3 and also Fig. 4. The interaction between amine groups in PAMAM and hydroxyl groups in lignin caused more resistant to high temperature. This indicates that lignin/PAMAM is more thermally stable than pristine lignin. In Table 4, the comparison between the first and second notable peaks in DTG has given indicates the positive effect of dendrimer and its rich functional group on thermal stability. This effect confirmed that using dendrimer in lignin mats could be a sufficient method for the production of carbon fiber from lignin and also high mechanical properties.

Preprints (www.preprints.org) | NOT PEER-REVIEWED | Posted: 28 July 2020 doi:10.20944/preprints202007.0671.v1

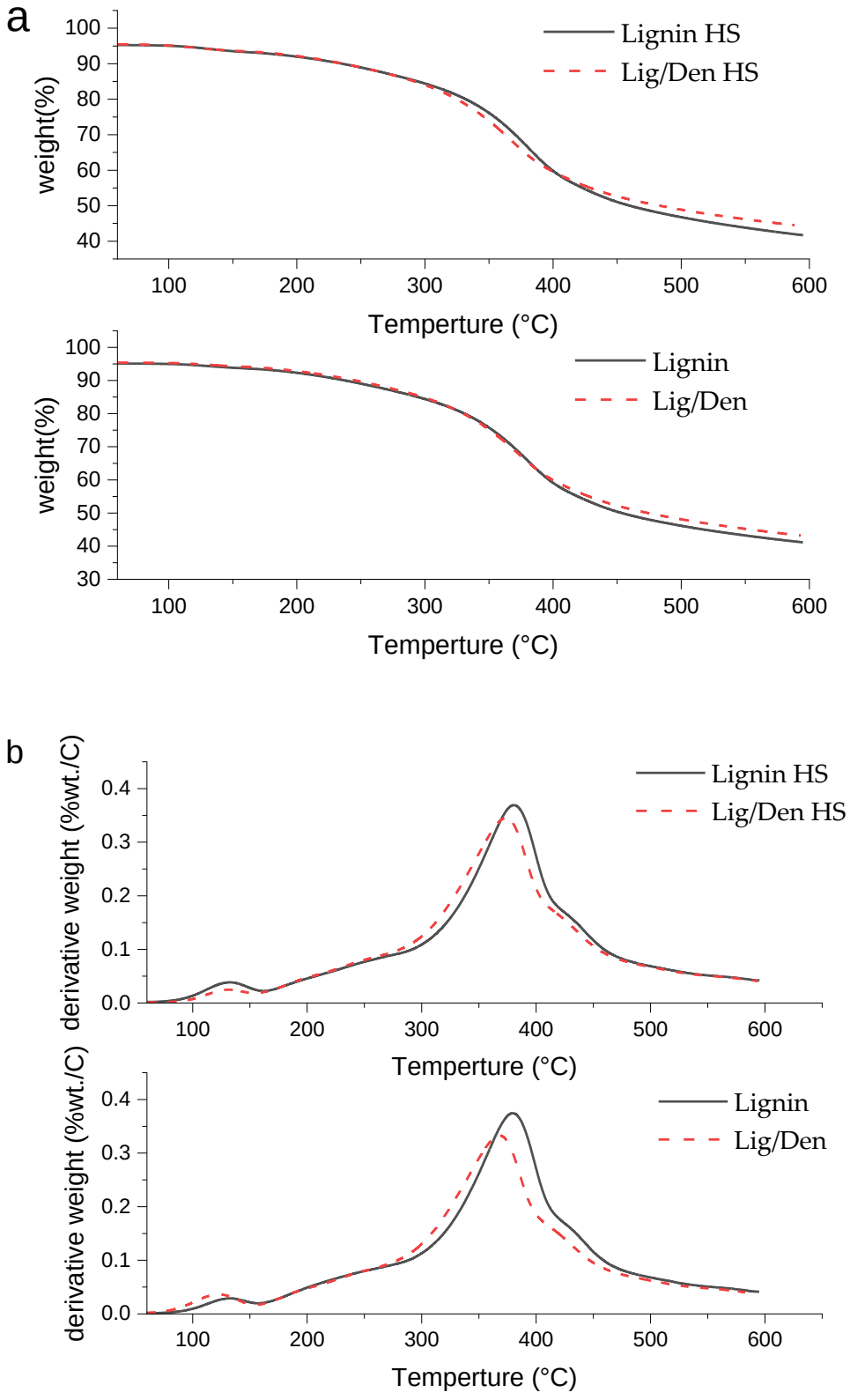


**Fig.4.** The TG (a) and DTG (b) curves of the lignin and lignin/PAMAM untreated and heat-set state (HS).

Preprints (www.preprints.org) | NOT PEER-REVIEWED | Posted: 28 July 2020 doi:10.20944/preprints202007.0671.v1

**Table 3.** The characteristic points of TG and DTG curve at two main peaks.

| component | $T_d$ [a] (°C) | %weight | $\alpha_1$ [b] | $\alpha_2$ [c] |
|---|---|---|---|---|
| Lignin | 595.53 | 41.12 | 0.374 | 0.029 |
| Lignin/PAMAM | 594.32 | 43.2 | 0.345 | 0.038 |
| Lignin (HS) | 596.20 | 41.69 | 0.369 | 0.024 |
| Lignin/PAMAM (HS) | 589.22 | 45.54 | 0.332 | 0.036 |

[a] The decomposition temperature.

[b] The derivative weight (%wt./C) at 66% weight.

[c] The derivative weight (%wt./C) at 94% weight.

*2.5 Fourier transform infrared spectroscopy (FTIR)*

Lignin has lots of functional groups due to its many different types of extraction and utilization. Therefore, it is often complicated to characterize all lignin and lignin based samples. As shown in Fig. 5, the important characteristic bands of lignin are revealed in Table 4. The peak at 1429-1509 and 1601 $cm^{-1}$ is related to C-C aromatic rings [57]. The lignin's alcohol picks appeared different bands (at 1260-1270 and 1330-1375 $cm^{-1}$) related to the guaiacyl and syringyl, respectively. In addition, the carbonyl group is seen at 1700-1715 $cm^{-1}$ [58]. The absorption bands of water appear in a range of 1300-1800 $cm^{-1}$ and 3500-3964 $cm^{-1}$. The existence of CO is elucidated at 2112 and 2180 $cm^{-1}$, while $CO_2$ appeared at 2217-2391 $cm^{-1}$ [56]. The most notable band in lignin is O–H due to the presence of the alcoholic and phenolic structure of lignin at 1300-1400$cm^{-1}$. The absorption bands at 2850-3200 $cm^{-1}$ indicate the hydrocarbons, such as methane [54]. On the other hand, PAMAM, which is rich in amine terminated functional group, produce pick bands at 1550-1640 $cm^{-1}$. The band at 3100-3500 $cm^{-1}$ is elucidated the amino groups of PAMAM. At 1630-1680 $cm^{-1}$ and these absorptions appeared in FTIR spectroscopy of lignin/PAMAM (Fig. 5) which is a proof to the reaction between lignin and PAMAM. As it has shown in Fig.5 (C), a new peak illustrated by No.4 confirm the reaction of amine group of PAMAM and hydroxyl group of lignin at 1485 $cm^{-1}$ [59]. Moreover, there are characteristic peaks of lignin in Fig.5 : (No.1) which indicates hydroxyl group at 1650 $cm^{-1}$, (No.2) that appear at 1600 $cm^{-1}$ according to aromatic rings, (No.3) which reveals at 1520 $cm^{-1}$ indicates C=C bonds and derivatives [58].

Preprints (www.preprints.org) | NOT PEER-REVIEWED | Posted: 28 July 2020 doi:10.20944/preprints202007.0671.v1

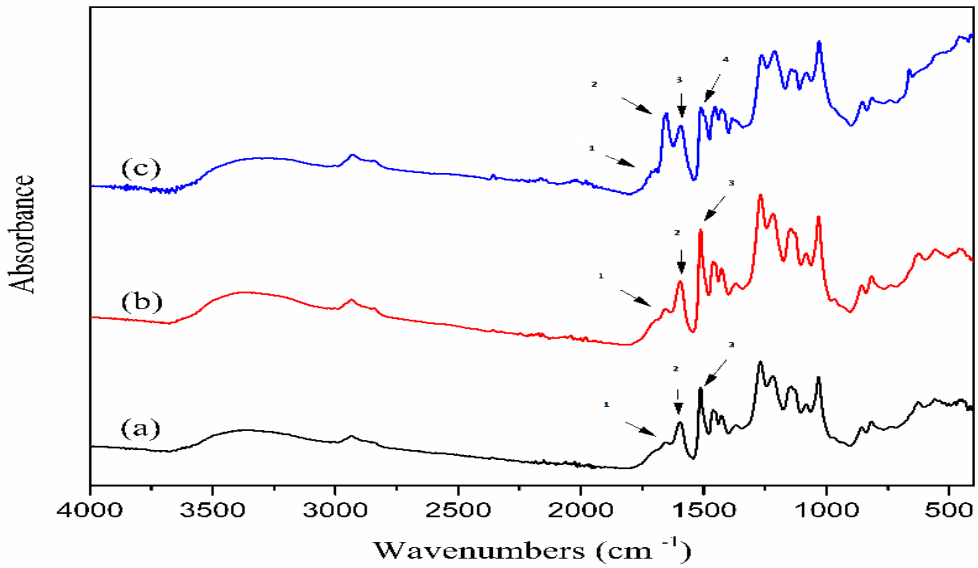


**Fig. 5.** FTIR spectra of (a)lignin (b)lignin/PAMAM 1wt% (c)lignin/PAMAM 2wt%.

**Table 4.** Main contents of different lignin samples and their range of evolution detected by FTIR.

| Wavenumber ($cm^{-1}$) | Functional group | Vibration | Compounds | Refs. |
|---|---|---|---|---|
| 645-690 | C=O | Dactyl-zone | | [55, 58] |
| 974-1058 | C–O | Stretching | R–OH | [55, 57] |
| 1000-1300 | C-O | Stretching | | [54, 58] |
| 1093-1188 | C–C | Skeleton | | [55] |
| 1310-1365 | $C–CH_3$ | Bending | Alkyls | [55, 58] |
| 1300-1400 | O–H | Bending | | [56, 57] |
| 1513 | C=C–OH | Stretching | | [58] |
| 1613 | C=C | Stretching | Aromatics | [58] |
| 1645-1750 | O–H | Bending | $H_2O$ | [55] |
| 2020-2220 | C–O | Stretching | CO | [55] |
| 2210-2390 | C=O | Stretching | $CO_2$ | [55, 58] |
| 2750-2990 | $C–H_2$ | Asymmetric Stretching | | [54, 55] |
| 2904-2979 | C–H | Stretching | | [57] |
| 2990-3010 | C–H | Stretching | | [54, 57] |
| 3020-3190 | C–H | Stretching | $CH_4$ | [56, 57] |
| 3500-3600 | O–H | Stretching | | [54, 57] |
| 3823-3870 | O–H | Stretching | | [55, 57] |

Preprints (www.preprints.org) | NOT PEER-REVIEWED | Posted: 28 July 2020 doi:10.20944/preprints202007.0671.v1

*2.6. Viscosity*

To reveal the interaction of lignin with PAMAM, lignin and lignin/PAMAM solutions were prepared and their viscosity measured in corresponding to time. Furthermore, due to the relationships between viscosity measurement and fiber diameter, the SEM images of the electrospun fibers after 5 days were also investigated. As general rules in polymeric solution, the viscosity would be increased subsequently by increasing more entanglement between polymeric chains, while it is reduced due to the less entanglement [60]. The viscosity of lignin and lignin/PAMAM in DMF solvent in 5 consecutive days were elucidated in Fig. 6. The result reveals that the viscosity for both lignin and lignin/PAMAM show increasing trend and then decreased. It seems that the unique structure of lignin, which has rich in phenolic rings and hydroxyl groups, cause the depolymerization of lignin in DMF. The structure causes higher viscosity. The viscosity of lignin just like other polymer reduced finally due to solution transition mechanism and reduction rate in radical polymerization in DMF due to the transfer reaction to solvent [61]. Also, the rate of free radical polymerization mechanism increases due to the radicals which react with lignin functional group and observed the increasing viscosity of lignin at first three days. After three days, the viscosity reduced due to the chain transfer to solvent. The viscosity measurement results in lignin/PAMAM solution is interesting due to the increase of solution viscosity. The interaction between PAMAM and lignin made the solution denser due to more molecular chain entanglement. The highest viscosities were 72 and 76.6 mPa.s for lignin and lignin/PAMAM, respectively.

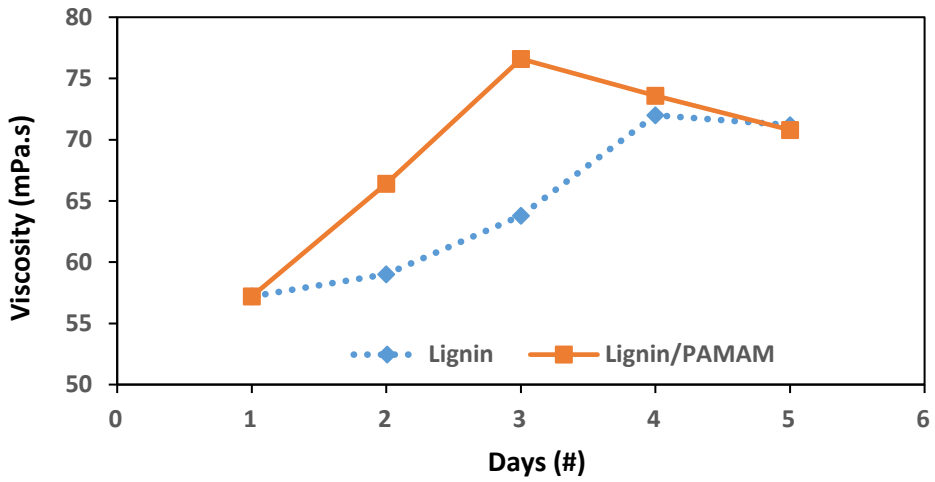


**Fig. 6.** The viscosity of lignin and lignin/PAMAM through 5 days.

Preprints (www.preprints.org) | NOT PEER-REVIEWED | Posted: 28 July 2020 doi:10.20944/preprints202007.0671.v1

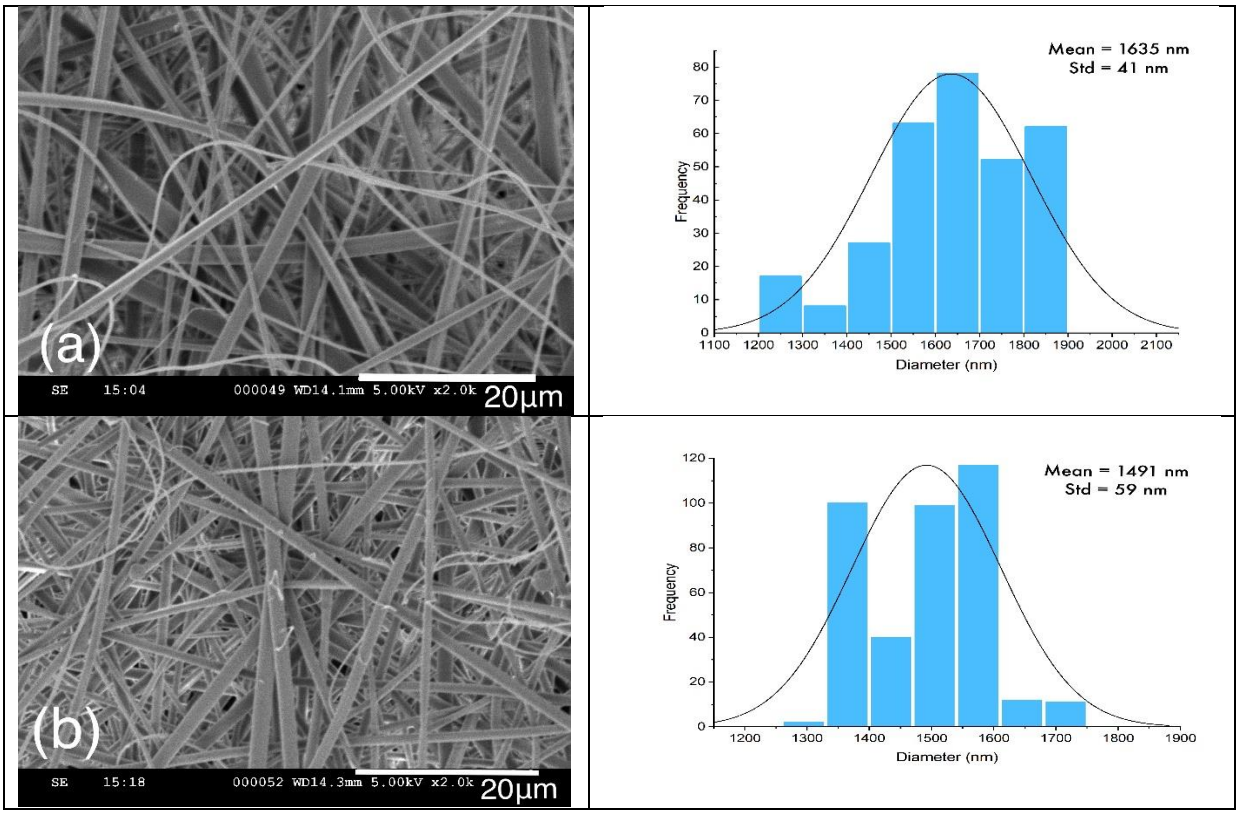


**Fig. 7.** SEM image and diameter distribution of (a) lignin and (b) lignin/PAMAM after 5 days.

*2.7 Reaction mechanism between lignin and amine-terminated dendrimer*

Despite of attempts made to define the various structural elements of lignin, the clear chemical structure of softwood kraft lignin (SKL) is still under investigation due to the complexity of various type [62]. Even though the most quantity of define structure belongs to the methoxy groups, SKL has various inter-unit bonds, such as *Arylglycerol-β-aryl ethers, Phenyl coumaran, Pinoresinols, Lignin carbohydrate α-benzyl ethers, Stilbenes, Aryl enol ethers, Secoisolariciresinols*, and end groups, such as *Cinnamyl alcohols, Arylacetic acid, Aryl-hydroxy-acetic acid, Aryl ethyl ketones, Aryl propanols, Aryl hydroxyethyl ketone, Aromatic aldehydes, Cinnamyl aldehydes*, and functional groups, such as *Aromatic C–H, Methoxy, Quinones*, and also hydroxyl groups, such as *Carboxylic OH, Aliphatic OH, o-Disubstituted phenols (including o-substituted catechols), o-Monosubstituted phenols, and phenolic OH* were figured out in SKL with different percentages [62]. It is well-known that, the amination reaction of lignin is regularly gone through Mannich reaction with amino group and formaldehyde [63]. In the absent of formaldehyde in lignin/PAMAM solutions, the reaction between PAMAM and main segment of lignin (methoxy groups) is carried out with hydrogen bonding and ionic interaction between hydroxyl group in lignin and amino terminated group in PAMAM. The regular reaction has been occurred between R-OH and R'-$NH_2$ which R and R' coming from the substitutions of lignin and PAMAM, respectively. The results of these interactions confirm by new peaks in FTIR, strength enhancement, and particularly viscosity after one week results in previous section.

Preprints (www.preprints.org) | NOT PEER-REVIEWED | Posted: 28 July 2020 doi:10.20944/preprints202007.0671.v1

Since it is very complicated to demonstrate the reaction between wood kraft lignin and PAMAM, the chemical interaction between Guaiacyl (G) lignin and lower generation, 1st generation, of PAMAM have been illustrated in Fig. 8.

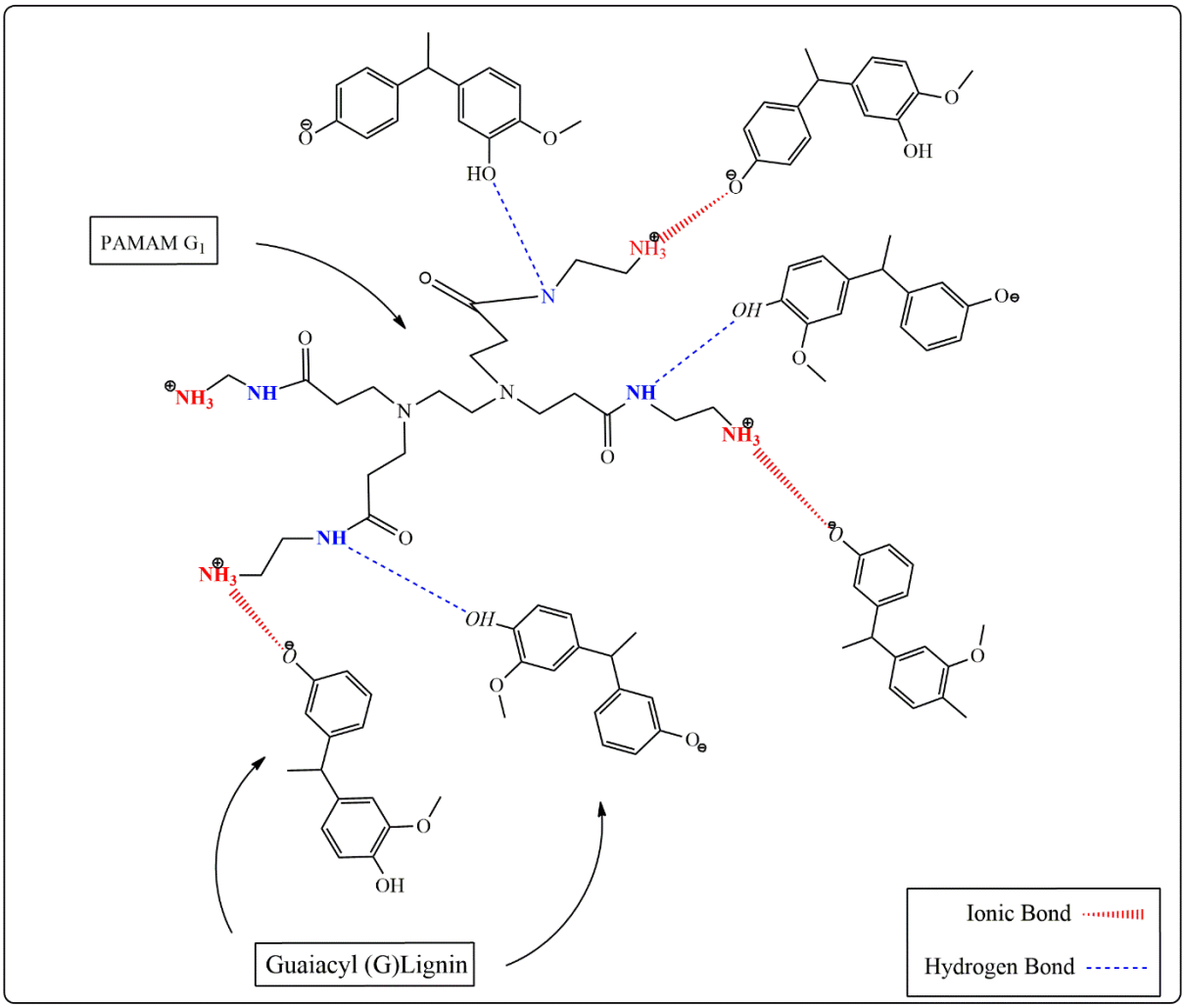


**Fig. 8.** The possible ionic and hydrogen bonding between lignin and PAMAM.

## 3. Materials and Methods

### *3.1. Materials*

Softwood Kraft Lignin (SKL) was supplied by FP Innovations (Vancouver, BC) and used with no further purification. N, N- Dimethylformamide (DMF, 99.9%), Polyethylene Oxide (PEO) ($M_w$ = 900 kDalton) was purchased from Aldrich. polyamidoamine (PAMAM) dendritic polymers was donated by Delta Innovative Company Poland.

### *3.2 Preparation and Properties of Electrospinning Solutions*

Preprints (www.preprints.org) | NOT PEER-REVIEWED | Posted: 28 July 2020 doi:10.20944/preprints202007.0671.v1

Electrospinning solutions were prepared by dissolving of exact amount of SKL into the DMF solvent in the presence of 1 wt. % PEO based on the lignin powder. For lignin/PAMAM samples, first 1 and 2 wt. % of PAMAM based on the lignin powder were dissolved in DMF solvent, while lignin and PEO separately dissolved in DMF solvent. After 2 hours mixing, these two solution mixing together and continue for another 1 hour before electrospinning. The solution concentration for all samples was 30 wt%. The electrospinning procedure has been applied in electrospinning distance of 15 cm at a point of an applied voltage range of 17kV and the 0.01 mL/min pump speed.

*3.2.1. Heat-setting and stabilization procedure*

After drying the mats at room temperature for 10 hours, for preparing the heat-set samples, the samples were heated in oven at air atmosphere to 150°C for 120 minutes. While, for stabilization procedure, the samples were heated at 4°C/min heating rate to 250°C for 90 minutes in a gas chromatography oven (Hewlett Packard 5890 Series II).

*3.3 Characterization of Composite Membranes*

*3.3.1 Morphology measurement*

The morphology of the electrospun nanofibrous mats was observed by a scanning electron microscope (SEM) (Hitachi S-2300) with an acceleration voltage of 5-20 kV. All of the samples were gold coated before SEM observation. The average diameter of nanofibers was determined by analyzing the SEM images via Image J software.

*3.3.2. Mechanical Properties*

The mechanical properties of the electrospun mats were evaluated using a multipurpose micro-tensile tester (KES-G1, Kato-Tech Co. Ltd) with a 5 kg capacity force transducer. Strip-specimens (0.5 cm W×5 cm L) were tested with 5 replications for each sample at a cross-head speed of 0.2 cm/s. The strain was calculated by dividing the displacement by the gauge length. Stress was obtained using the following formula:

$$\sigma_{specific} = \text{Specific Stress (N/Tex)} = \frac{Force(N)/Width\ of\ specimen\ (mm)}{Areal\ density\ of\ specimen\ (g/sq.M)}$$

1N/tex = 145,000 psi = 1 GPa

Load cell setting was g/10v, deformation rate was set at 0.02 cm/s, the specimen length was 5 cm, and the mass of specimen was calculated separately for each sample. The engineering stress $\sigma_{Eng}$ was achieved from the equations below (where $V$ represent the signal voltage read through the machine):

$$Deformation(cm) = Deformation\ rate \times \Delta t$$

$$Strain\ \left(\frac{cm}{cm}\right) = \frac{defromation}{specimen\ length}$$

Preprints (www.preprints.org) | NOT PEER-REVIEWED | Posted: 28 July 2020 doi:10.20944/preprints202007.0671.v1

$$Load(g) = Load\ cell\ setting\ \times \Delta V$$

Areal density was calculated as:

$$Areal\ Density\left(\frac{g}{m^2}\right) = \frac{Sample\ Mass(g)}{length(m) \times width(m)}, \quad \sigma_{specific}\left(\frac{g}{tex}\right) = \frac{load(g)}{Areal\ Density\left(\frac{g}{m^2}\right) \times Width(mm)}$$

Converting the specific stress to engineering stress can be achieved by:

$$\sigma_{Eng}(MPa) = \sigma_{specific}\left(\frac{g}{tex}\right) \times 9.81 \times \rho_{polymer}\ (g/cm^3)$$

*3.3.3. Surface charge*

The Surface Zeta Potential (SZP) electrode was used for analyzing the charge on a fibrous mats surface by NanoBrook instrument Brookhaven Instruments Corporation 750 Blue Point Road, Holtsville, NY 11742. Measurements were accomplished by attaching the sample to a horizontal place situated perpendicularly between two electrodes. The sample and electrodes were placed into a diluent containing probe particles for which the charge is well-known.

*3.3.4. Thermogravimetric analysis (TGA)*

Thermogravimetry is a method to recognize the thermal resistance of the sample and its components to obtain useful properties like oxidative degradation, dissolution, decomposition [64]. Thermogravimetric analysis (TGA) was carried out on a thermogravimetric analyzer (Q500, TA Instruments, USA). Samples were heated at 20 °C/min from room temperature to 600 °C in a dynamic nitrogen atmosphere (flow rate = 60 ml/min).

*3.3.5 Fourier transform infrared spectroscopy (FTIR)*

Fourier transform infrared spectroscopy (FTIR) can provide important information on the molecular structure of components and has been used mainly for chemical characterization of geological samples recently [65-67]. The mechanism of the FTIR technique is related to transitions between quantized vibrational energy states[65, 68]. The FTIR spectra were recorded over the range 400-4000cm$^{-1}$ with 64 scans and the resolution of 4 cm$^{-1}$.

*3.3.6 Viscosity measurement*

The solution viscosity of lignin for electrospinning is an essential factor that should be considered and controlled. The concentration of lignin in the solution and time are the main two elements that affect the viscosit [69, 70]. In this study, dimethylformamide (DMF) was the solvent, and all experiments were applied on lignin/DMF and lignin/PAMAM/DMF solution. The effect of time

the mixing on the viscosity measurement through 5 days was determined. The viscosity reported by the torsional oscillation-type viscometer, SEKONIK corporation, VM 10A series Nerima-ku, Tokyo, 178-8686 Japan.

## 4. Conclusions

The blending of softwood kraft lignin and PAMAM dendritic polymers, and electrospinning of the resulting blends were demonstrated in this paper. Heat-setting and stabilization procedure were applied to both lignin and lignin/PAMAM mats. The chemical interaction between hydroxyl groups in lignin-based mats and amino functional groups in PAMAM dendritic structures were systematically confirmed by FTIR and viscosity measurement. Increasing surface charge of lignin/PAMAM was another evidence for the demonstrating interaction between cationic amino groups in PAMAM and lignin products. There was more than 45% enhancement in breaking stress for lignin/PAMAM mats comparing to lignin mats, while an approximately 20% improvement was obtained for untreated mats. The reduction in fiber diameter for lignin/PAMAM fiber was found as a result of higher surface tension of the solution in PAMAM lignin. Such enhancements in mechanical and chemical properties of lignin/PAMAM fibers could provide an encouraging strategy for strength improvement during the future development of low cost precursors for multifunctional lignin fiber-based products, such as those for filtration.

## Acknowledgement

The authors would like to thank MITACS for their financial support of the project. Thanks are due to Mr. Hekun Kuang for his assistance with the tenacity testing. The funding of equipment provided by the Canada Foundation for Innovation (CFI) is greatly appreciated.

## References

1. Faruk, O. and M. Sain, *Lignin in polymer composites*. 2015: William Andrew.
2. Pouteau, C., et al., *Lignin–polymer blends: evaluation of compatibility by image analysis.* Comptes rendus biologies, 2004. **327**(9-10): p. 935-943.
3. Zhang, F., et al., *Optimization of Trichoderma harzianum T-E5 biomass and determining the degradation sequence of biopolymers by FTIR in solid-state fermentation.* Industrial crops and products, 2013. **49**: p. 619-627.
4. Boerjan, W., J. Ralph, and M. Baucher, *Lignin biosynthesis.* Annual review of plant biology, 2003. **54**(1): p. 519-546.
5. Kumar, M., M. Hietala, and K. Oksman, *Lignin-based Electrospun Carbon Nanofibers.* Frontiers in Materials, 2019. **6**: p. 62.
6. La Cruz, D. and F. Banaag, *Fate and Reactivity of Lignin in Municipal Solid Waste (MSW) Landfill.* 2013.
7. Dence, C. and S. Lin, *Lignin determination.* Methods in Lignin Chemistry, 1992. **33**: p. 61.
8. dos Santos, P.S., et al., *Characterisation of Kraft lignin separated by gradient acid precipitation.* Industrial Crops and Products, 2014. **55**: p. 149-154.

9. Bertella, S. and J.S. Luterbacher, *Lignin Functionalization for the Production of Novel Materials.* Trends in Chemistry, 2020.
10. Guerra, A., et al., *On the propensity of lignin to associate: A size exclusion chromatography study with lignin derivatives isolated from different plant species.* Phytochemistry, 2007. **68**(20): p. 2570-2583.
11. Ugartondo, V., M. Mitjans, and M.P. Vinardell, *Comparative antioxidant and cytotoxic effects of lignins from different sources.* Bioresource technology, 2008. **99**(14): p. 6683-6687.
12. Qian, Y., X. Qiu, and S. Zhu, *Lignin: a nature-inspired sun blocker for broad-spectrum sunscreens.* Green Chemistry, 2015. **17**(1): p. 320-324.
13. Glasser, W.G., R.A. Northey, and T.P. Schultz, *Lignin: historical, biological, and materials perspectives*. 1999: ACS Publications.
14. Beaucamp, A., et al., *Carbon fibres from renewable resources: the role of the lignin molecular structure in its blendability with biobased poly (ethylene terephthalate).* Green Chemistry, 2019. **21**(18): p. 5063-5072.
15. Boudet, A.M., et al., *Lignins and lignocellulosics: a better control of synthesis for new and improved uses.* Trends in plant science, 2003. **8**(12): p. 576-581.
16. Kadla, J., et al., *Lignin-based carbon fibers for composite fiber applications.* Carbon, 2002. **40**(15): p. 2913-2920.
17. Gul, V., E. Lyubeshkina, and A. Shargorodskii, *Mechanical properties of polypropylene modified by decomposition products of alkali sulfate lignin.* Polymer Mechanics, 1965. **1**(6): p. 1-4.
18. Košíková, B., M. Kačuráková, and V. Demianova, *Photooxidation of the composite lignin/polypropylene films.* Chemical Papers, 1993. **47**(2): p. 132-136.
19. Rodrigues, P.C., et al., *Polyaniline/lignin blends: FTIR, MEV and electrochemical characterization.* European Polymer Journal, 2002. **38**(11): p. 2213-2217.
20. Baumberger, S., C. Lapierre, and B. Monties, *Utilization of pine kraft lignin in starch composites: impact of structural heterogeneity.* Journal of agricultural and food chemistry, 1998. **46**(6): p. 2234-2240.
21. Sarkanen, K.V. and C.H. Ludwig, *Liguins. Occurrence, formation, structure, and reactions*. 1971.
22. Wu, R., et al., *Preparation, structure, and properties of poly (ethyleneoxide)/lignin composites used for UV absorption.* Journal of Applied Polymer Science, 2020. **137**(16): p. 48593.
23. Bu, L., et al., *Comparison of hydrophilic variation and bioethanol production of furfural residues after delignification pretreatment.* Bioscience, biotechnology, and biochemistry, 2014. **78**(8): p. 1435-1443.
24. Park, Y., W.O. Doherty, and P.J. Halley, *Developing lignin-based resin coatings and composites.* Industrial crops and products, 2008. **27**(2): p. 163-167.
25. Kirk, T.K. and J.R. Obst, *Lignin determination*, in *Methods in enzymology*. 1988, Elsevier. p. 87-101.
26. Cateto, C.A., et al., *Kinetic study of the formation of lignin-based polyurethanes in bulk.* Reactive and Functional Polymers, 2011. **71**(8): p. 863-869.
27. Akbari, S. and R.M. Kozłowski, *A review of application of amine-terminated dendritic materials in textile engineering.* The journal of the Textile Institute, 2019. **110**(3): p. 460-467.
28. Seiler, M., *Hyperbranched polymers: Phase behavior and new applications in the field of chemical engineering.* Fluid Phase Equilibria, 2006. **241**(1-2): p. 155-174.
29. Ruiz-Rosas, R., et al., *The production of submicron diameter carbon fibers by the electrospinning of lignin.* Carbon, 2010. **48**(3): p. 696-705.
30. Dallmeyer, I., F. Ko, and J.F. Kadla, *Electrospinning of technical lignins for the production of fibrous networks.* Journal of Wood Chemistry and Technology, 2010. **30**(4): p. 315-329.

31. Poursorkhabi, V., A.K. Mohanty, and M. Misra, *Electrospinning of aqueous lignin/poly (ethylene oxide) complexes.* Journal of Applied Polymer Science, 2015. **132**(2).
32. Seo, D.K., et al., *Preparation and characterization of the carbon nanofiber mat produced from electrospun PAN/lignin precursors by electron beam irradiation.* Rev. Adv. Mater. Sci, 2011. **28**(1): p. 31-34.
33. Ago, M., et al., *Lignin-based electrospun nanofibers reinforced with cellulose nanocrystals.* Biomacromolecules, 2012. **13**(3): p. 918-926.
34. Dallmeyer, I., et al., *Preparation and Characterization of Interconnected, Kraft Lignin-B ased Carbon Fibrous Materials by Electrospinning.* Macromolecular Materials and Engineering, 2014. **299**(5): p. 540-551.
35. Bahi, A., et al., *Membranes based on electrospun lignin-zeolite composite nanofibers.* Separation and Purification Technology, 2017. **187**: p. 207-213.
36. Kim, S. and B.E. Dale, *Global potential bioethanol production from wasted crops and crop residues.* Biomass and bioenergy, 2004. **26**(4): p. 361-375.
37. Pourmoazzen, Z., et al., *Cholesterol-modified lignin: A new avenue for green nanoparticles, meltable materials, and drug delivery.* Colloids and Surfaces B: Biointerfaces, 2020. **186**: p. 110685.
38. Lora, J.H. and W.G. Glasser, *Recent industrial applications of lignin: a sustainable alternative to nonrenewable materials.* Journal of Polymers and the Environment, 2002. **10**(1-2): p. 39-48.
39. Ramakrishna, S., *An introduction to electrospinning and nanofibers*. 2005: World Scientific.
40. Ebers, L.-S., et al., *Impact of PEO structure and formulation on the properties of a Lignin/PEO blend.* Industrial Crops and Products, 2020. **143**: p. 111883.
41. Yang, M., et al., *Preparation of lignin containing cellulose nanofibers and its application in PVA nanocomposite films.* International Journal of Biological Macromolecules, 2020.
42. Cui, M., et al., *Rigid oligomer from lignin in designing of tough, self-healing elastomers.* ACS Macro Letters, 2018. **7**(11): p. 1328-1332.
43. Brosse, N., et al., *Investigation of the chemical modifications of beech wood lignin during heat treatment.* Polymer Degradation and Stability, 2010. **95**(9): p. 1721-1726.
44. Kim, J.-Y., et al., *Investigation of structural modification and thermal characteristics of lignin after heat treatment.* International journal of biological macromolecules, 2014. **66**: p. 57-65.
45. Aslanzadeh, S., et al., *Morphologies of electrospun fibers of lignin in poly (ethylene oxide)/N, N-dimethylformamide.* Journal of Applied Polymer Science, 2016. **133**(44).
46. Ali Mohammadpoor, S., et al., *Fabrication of electrospun ibuprofen-loaded poly (vinyl alcohol)/hyper-branched poly (ethylenimine) fibers and their release behaviors.* Journal of Biomaterials Science, Polymer Edition, 2020. **31**(2): p. 261-275.
47. Norberg, I., *Carbon fibres from kraft lignin*. 2012, KTH Royal Institute of Technology.
48. Jämsä, S. and P. Viitaniemi. *Heat treatment of wood–Better durability without chemicals*. in *Proceedings of special seminar held in Antibes, France*. 2001.
49. Yildiz, S., E.D. Gezer, and U.C. Yildiz, *Mechanical and chemical behavior of spruce wood modified by heat.* Building and environment, 2006. **41**(12): p. 1762-1766.
50. Klapiszewski, Ł., et al., *Physicochemical and electrokinetic properties of silica/lignin biocomposites.* Carbohydrate polymers, 2013. **94**(1): p. 345-355.
51. Kuzniatsova, T., et al., *Zeta potential measurements of zeolite Y: Application in homogeneous deposition of particle coatings.* Microporous and mesoporous materials, 2007. **103**(1-3): p. 102-107.
52. Bernsmann, F., et al., *Protein adsorption on dopamine–melanin films: Role of electrostatic interactions inferred from ζ-potential measurements versus chemisorption.* Journal of colloid and interface science, 2010. **344**(1): p. 54-60.

53. Faleva, A.V., et al., *Structural characteristics of different softwood lignins according to 1D and 2D NMR spectroscopy.* Journal of Wood Chemistry and Technology, 2020. **40**(3): p. 178-189.
54. Liu, Q., et al., *Mechanism study of wood lignin pyrolysis by using TG–FTIR analysis.* Journal of Analytical and Applied Pyrolysis, 2008. **82**(1): p. 170-177.
55. Shen, D., et al., *The pyrolytic degradation of wood-derived lignin from pulping process.* Bioresource technology, 2010. **101**(15): p. 6136-6146.
56. Fenner, R.A. and J.O. Lephardt, *Examination of the thermal decomposition of kraft pine lignin by Fourier transform infrared evolved gas analysis.* Journal of agricultural and food chemistry, 1981. **29**(4): p. 846-849.
57. Fengel, D. and G. Wegener, *Wood: chemistry, ultrastructure, reactions*. 2011: Walter de Gruyter.
58. Pasquali, C.L. and H. Herrera, *Pyrolysis of lignin and IR analysis of residues.* Thermochimica Acta, 1997. **293**(1-2): p. 39-46.
59. Mohseni, M., et al., *Amine-terminated dendritic polymers as a multifunctional chelating agent for heavy metal ion removals.* Environmental Science and Pollution Research, 2019. **26**(13): p. 12689-12697.
60. Gedde, U., *Polymer physics*. 1995: Springer Science & Business Media.
61. Dong, D. and A.L. Fricke, *Intrinsic viscosity and the molecular weight of kraft lignin.* Polymer, 1995. **36**(10): p. 2075-2078.
62. Crestini, C., et al., *On the structure of softwood kraft lignin.* Green Chemistry, 2017. **19**(17): p. 4104-4121.
63. Matsushita, Y. and S. Yasuda, *Reactivity of a condensed–type lignin model compound in the Mannich reaction and preparation of cationic surfactant from sulfuric acid lignin.* Journal of wood science, 2003. **49**(2): p. 166-171.
64. Coats, A. and J. Redfern, *Thermogravimetric analysis. A review.* Analyst, 1963. **88**(1053): p. 906-924.
65. Chen, Y., et al., *Applications of micro-fourier transform infrared spectroscopy (FTIR) in the geological sciences—a review.* International journal of molecular sciences, 2015. **16**(12): p. 30223-30250.
66. von Aulock, F.W., et al., *Advances in Fourier transform infrared spectroscopy of natural glasses: From sample preparation to data analysis.* Lithos, 2014. **206**: p. 52-64.
67. Rossman, G.R., *Analytical methods for measuring water in nominally anhydrous minerals.* Reviews in Mineralogy and Geochemistry, 2006. **62**(1): p. 1-28.
68. Gao, J., et al., *Spectrum Reconstruction of a Spatially Modulated Fourier Transform Spectrometer Based on Stepped Mirrors.* Applied spectroscopy, 2017. **71**(6): p. 1348-1356.
69. Giummarella, N., et al., *Lignin prepared by ultrafiltration of black liquor: Investigation of solubility, viscosity, and ash content.* BioResources, 2016. **11**(2): p. 3494-3510.
70. Cho, M., et al., *Enhancement of the mechanical properties of electrospun lignin-based nanofibers by heat treatment.* Journal of Materials Science, 2017. **52**(16): p. 9602-9614.